EurJIC European Journal of Inorganic Chemistry

FULL PAPER

DOI: 10.1002/ejic.201200212

# Photoinitiated Dioxygenase-Type Reactivity of Open-Shell 3d Divalent Metal Flavonolato Complexes

Katarzyna Grubel,[a] Amy R. Marts,[b] Samuel M. Greer,[b] David L. Tierney,[b] Caleb J. Allpress,[a] Stacey N. Anderson,[a] Brynna J. Laughlin,[c] Rhett C. Smith,[c] Atta M. Arif,[d] and Lisa M. Berreau*[a]

**Keywords:** Bioinorganic chemistry / Enzyme models / Homogeneous catalysis / Oxygen / Carbon monoxide

Irradiation of 3-hydroxyflavonolato (3-Hfl) complexes of $Mn^{II}$, $Co^{II}$, $Ni^{II}$ and $Cu^{II}$, supported by the 6-$Ph_2$TPA ligands **1**–**4**, at 300 nm under aerobic conditions, results in dioxygenase-type reactivity and the formation of the corresponding divalent metal *O*-benzoylsalicylato (*O*-bs) complexes **8**–**11** and CO. The latter were characterized by using multiple methods, including elemental analysis, X-ray crystallography, NMR and/or EPR spectroscopy, mass spectrometry and IR spectroscopy. Compounds **1**–**4** serve as catalysts for the photoinduced reactivity of 3-hydroxyflavonol (3-HflH) to produce *O*-benzoylsalicylic acid as the major product. Spectroscopic studies (UV/Vis and $^1$H NMR) show that each *O*-benzoylsalicylato complex **8**–**11** reacts with one equiv. of 3-hydroxyflavonol to regenerate **1**–**4** and enable turnover reactivity. Unlike what is observed for free 3-HflH, photoinduced reactions involving **1**–**4** and excess flavonol show only minor amounts of flavonol isomerization reactivity. These results indicate that the presence of a metal ion, whether under stoichiometric or catalytic conditions, facilitates the photoinduced degradation of 3-HflH to produce a carboxylic acid and CO as products.

## Introduction

Flavonoids are naturally occurring molecules found in plants. The chemistry of molecules of this class is of considerable current interest due to their antimicrobial, antioxidative and UV-protective properties.[1] 3-Hydroxyflavonol (3-HflH, Figure 1, top) is a flavonoid, although it is not found naturally in plants. This molecule has been used as an analog for the naturally occurring flavonoid quercetin (Figure 1, bottom) in model studies of relevance to quercetin dioxygenases.[2,3] These enzymes, which are found in fungi and bacteria, catalyze the oxidative ring-opening of quercetin, a reaction which results in the release of one equiv. of CO (Figure 1, bottom) and the formation of a carboxylic acid (termed a depside).[4,5] Notably, quercetinases have been found to utilize different 3d metal ions depending on the source.[4,5] Specifically, enzymes from fungi contain $Cu^{II}$, while the bacterial enzyme from *Streptomyces sp. FLA* exhibits highest activity with $Ni^{II}$ or $Co^{II}$ as the active site metal ion.

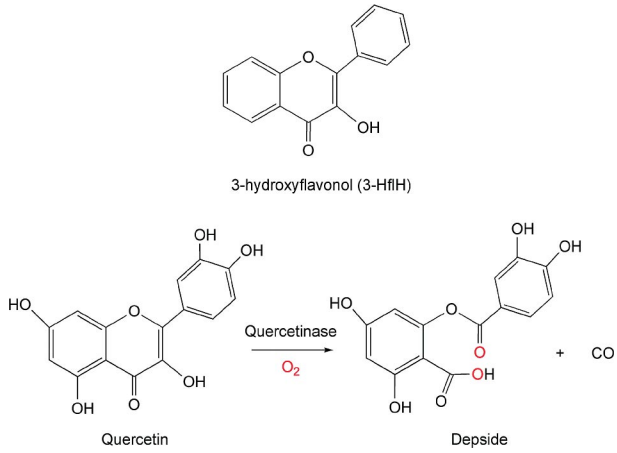


Figure 1. Top: structure of 3-hydroxyflavonol (3-HflH). Bottom: structure of quercetin and reaction catalyzed by quercetinase enzymes.

Several investigations of the thermally induced oxidative cleavage reactivity of copper flavonolato complexes have been reported.[2,3] Recently, similar studies have been reported for mononuclear $Mn^{II}$ and $Fe^{III}$ flavonolate species.[3] However, it should be noted that to date, no series of structurally similar 3-hydroxyflavonolato (3-Hfl) complexes has been examined in terms of oxidative cleavage reactivity, thus the influence of the metal ion cannot be clearly evaluated. We recently reported the first series of structurally related 3-Hfl complexes of 3d metals (**1**–**5**, Figure 2).[6] We

[a] Department of Chemistry & Biochemistry, Utah State University,
Logan, UT, USA
Fax: +1-435-797-3390
E-mail: lisa.berreau@usu.edu
[b] Department of Chemistry & Biochemistry, Miami University, Oxford, OH, USA
[c] Department of Chemistry, Clemson University, Clemson, SC, USA
[d] Department of Chemistry, University of Utah, Salt Lake City, UT, USA

Supporting information for this article is available on the WWW under http://dx.doi.org/10.1002/ejic.201200212.

  

have also prepared a structurally similar series for the Group 12 metal ions (**5**–**7**, Figure 2)[7] and have discovered that the latter complexes undergo clean photoinduced dioxygenase-type reactivity with release of CO when irradiated at 300 nm. This chemistry is new in that photoinduced oxidative ring opening and CO-release had not been previously reported for divalent metal flavonolato complexes.[8] We are interested in examining whether such reactivity may be used toward the development of new CO-releasing molecules (CORMs),[9] as such molecules are of current interest in potential therapeutic applications.[10]

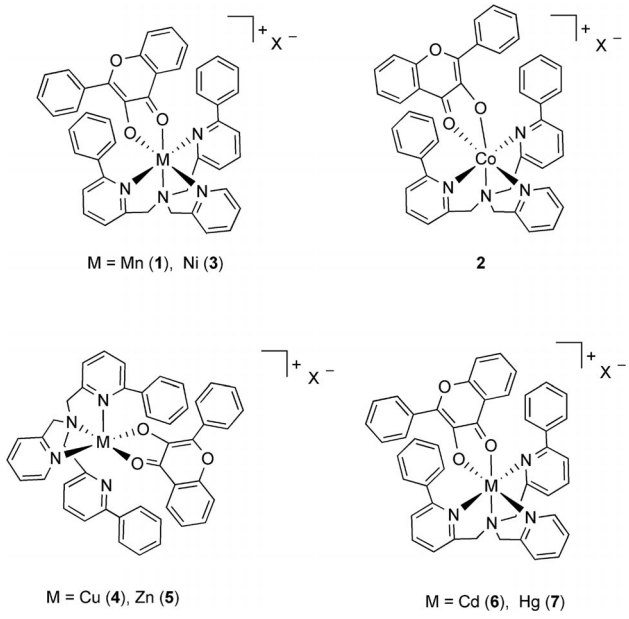


Figure 2. Structural features of **1**–**7**. X = $ClO_4^-$ or $OTf^-$.

Herein we report studies of the photoinduced oxidative ring-opening reactivity of the 3-Hfl complexes **1**–**4** (Figure 2). While undergoing dioxygenase-type CO release reactions similar to those found for **5**–**7**, lower reaction quantum yields result from quenching of the excited state by the open-shell $d^n$ metal ion. In the presence of excess 3-HflH, complexes **1**–**4** serve as catalysts to promote photoinduced catalytic oxidative flavonol ring-opening reactivity. These combined results indicate that the presence of a metal center, whether under stoichiometric or catalytic conditions, facilitates the photoinduced degradation of 3-HflH to produce a carboxylic acid and CO as products.

## Results and Discussion

### Spectroscopic Properties and Photoinduced Reactivity of 1–4. Characterization of the *O*-Benzoylsalicylato (*O*-bs) Complexes 8–11

The absorption spectra of **1**–**4** are shown in the Supporting Information (Figure S1). Free 3-hydroxyflavonol (3-HflH) in methanol exhibits three absorption bands at 240, 304 and 343 nm.[11] Complexes **1**–**4** exhibit a prominent absorption band in the region of 420–443 nm, as well as additional absorption features below 350 nm. Irradiation of an acetonitrile solution of each complex at 420 nm produces an emission band at approximately 475 nm (Supporting Information, Figures S2–S5). Similar emission features were found for **5**–**7**. However, the overall emission intensity is lower for **1**–**4** due to quenching of the excited state by the open $3d^n$ shell metal center.[12] Complexes **1**–**4** exhibit a fluorescence quantum yield of 0.00(1) ($Co^{II}$, $Ni^{II}$, $Cu^{II}$) or 0.02(1) ($Mn^{II}$) and a fluorescence lifetime of 1–2 ns.

Irradiation of $O_2$-purged solutions of **1**–**4** at 300 nm using a Rayonet photoreactor (ca. 35 °C) for 18 h results in the gradual loss of the absorption band at approximately 420 nm for each complex. Control reactions carried out in the dark indicate that the reactions taking place are photoinduced and not the result of heating of the samples in the photoreactor. The quantum yield for each reaction (**1**, **2** and **4**: $\phi = 0.005$; **3**: $\phi = 0.008$) was determined by actinometry using ferrioxalate as a standard to measure photon flux.[13] Sampling of the headspace gas of each reaction by GC and by means of the $PdCl_2$ method[13] ■■ ((<=Author: ref. [14]? we could not find the link to ref 14)) ■■ indicated the formation of CO. A yield of approximately 50% for one equiv. of CO was determined by GC from the reaction involving **3**. We attribute this less than quantitative yield to partitioning between the solvent and headspace of the reaction vessel and to possible loss of CO during the 18 h of irradiation required for the reaction to reach completion. Following work-up, the *O*-benzoylsalicylato (*O*-bs) complexes [(6-$Ph_2$TPA)M(*O*-bs)]$ClO_4$ (**8**–**11**) were characterized by elemental analysis, X-ray crystallography (**9**·0.25$CH_3CN$), FTIR, $^1$H NMR (**9** and **10**) and/or EPR (**8**, **9**, and **11**) spectroscopy and mass spectrometry. Complexes **8**–**11** represent the first species of relevance to potential product-bound forms of bacterial $Mn^{II}$, $Co^{II}$ and $Ni^{II}$ reconstituted quercentinases.[3,5a,15]

The cationic portion of **9**·0.25$CH_3CN$ is shown in Figure 3. Details of the data collection are given in Table 3. Selected bond lengths and angles are given in Table 1. The geometry of the $Co^{II}$ center is distorted trigonal bipyramidal ($\tau = 0.80$)[16] with the *O*-bs ligand exhibiting

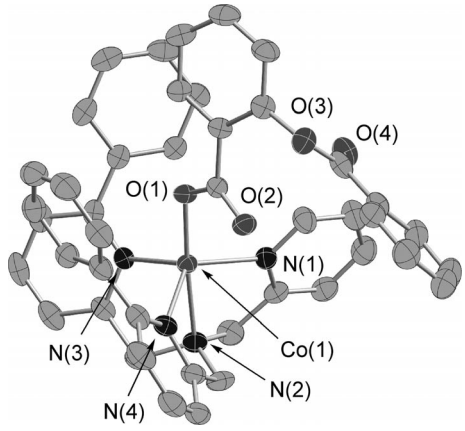


Figure 3. Thermal ellipsoid representation of the cationic portion of **9**·0.25$CH_3CN$. Ellipsoids are plotted at the 50% probability level. Hydrogen atoms have been omitted for clarity.

  

monodentate coordination in the axial position. The $Co^{II}$–N(PhPy) and Co–N(Py) bonds are similar to those found in the $Co^{II}$ flavonolato complex **2**.[6]

Table 1. Selected bond lengths [Å] and angles [°] for the cationic portion of **9**·0.25$CH_3CN$.

| | | | |
|---|---|---|---|
| Co(1)–O(1) | 1.9460(17) | O(1)–Co(1)–N(1) | 100.35(8) |
| Co(1)–N(1) | 2.105(2) | O(1)–Co(1)–N(4) | 105.73(8) |
| Co(1)–N(2) | 2.177(2) | N(1)–Co(1)–N(4) | 123.49(9) |
| Co(1)–N(3) | 2.120(2) | O(1)–Co(1)–N(3) | 106.01(8) |
| Co(1)–N(4) | 2.110(2) | N(1)–Co(1)–N(3) | 110.42(9) |
| N(1)–Co(1)–N(2) | 76.53(9) | N(4)–Co(1)–N(2) | 74.92(9) |
| N(3)–Co(1)–N(2) | 76.91(9) | | |

Complexes **9** and **10** are high-spin $Co^{II}$ and $Ni^{II}$ derivatives, respectively, that are amenable to investigation by $^1H$ NMR spectroscopy using paramagnetic parameters. The spectroscopic features of analytically pure **9** are shown in Figure 4 (middle), along with the spectroscopic feature of the flavonolato-$Co^{II}$ complex [(6-$Ph_2$TPA)Co(3-Hfl)]$ClO_4$ (**2**, Figure 4, top). A full assignment of ligand-based resonances in the spectra of **2** and **9** has not been performed. However, the pattern of resonances exhibited by the compounds is sufficiently different to indicate that $^1H$ NMR will be useful in examining interconversions of these compounds (vide infra). The $^1H$ NMR spectra of the $Ni^{II}$ flavonolato and *O*-bs complexes **3** and **10** are shown in the top and middle portions of Figure 5, respectively. Based on prior $^1H$ NMR studies of the 6-$Ph_2$TPA ligand supported $Ni^{II}$ complexes, assignment of the β, β′ and γ protons of the pyridyl rings can be made on the basis of chemical shift and relative intensity.[17] The features of the *O*-bs complex **10** in the region of 30–55 ppm are generally similar to those exhibited by the benzoate complex [(6-$Ph_2$TPA)Ni($O_2$CPh)]$ClO_4$, the structure of which contains a bidentate benzoate ligand.[18]

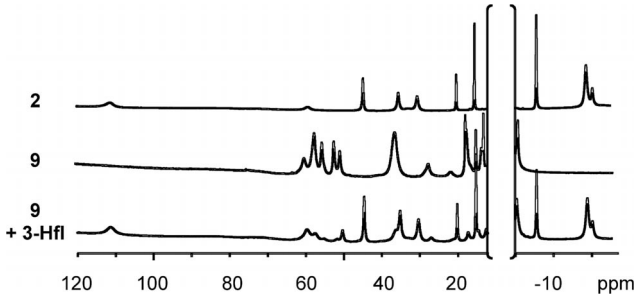


Figure 4. Features of the $^1H$ NMR spectra of [(6-$Ph_2$TPA)Co(3-Hfl)]$ClO_4$ (**2**, top), [(6-$Ph_2$TPA)Co(*O*-bs)]$ClO_4$ (**9**, middle) and **9** upon treatment with one equiv. of 3-Hfl in $CD_3CN$ (bottom).

We have also evaluated the EPR spectroscopic properties of **8**, **9** and **11** by means of comparison with their starting divalent metal flavonolato complexes. EPR spectra of the $Mn^{II}$ complexes **1** and **8** show complicated patterns centered at $g = 2$, with strong signals from the outer (5/2–3/2, 3/2–1/2, etc.) transitions (Figure 6, left), indicative of weak axial zero-field splittings ($D < h\nu$, $h\nu \approx 0.3$ cm$^{-1}$) in an environment that deviates from cubic symmetry. The positions of the outer transitions are nearly identical for the two complexes, suggesting that the magnitude of $D$ is largely unchanged, although they are dramatically different in intensity, with the six-coordinate $Mn^{II}$ flavonolato complex **1** showing a stronger response than the corresponding *O*-bs-$Mn^{II}$ complex. In addition to the lower outer transition intensity, the resolution of the central six-line pattern at $g = 2$ is also reduced in the *O*-bs complex, although the magnitude of the $^{55}Mn$ hyperfine coupling is unchanged (Figure 6, right). In both complexes $A(^{55}Mn) \approx 77$ G is substantially less than observed for hydrated $Mn^{II}$ (ca. 92 G).

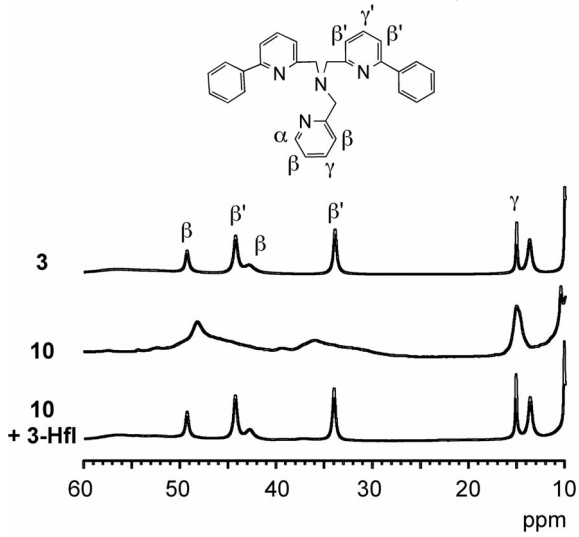


Figure 5. Features of the $^1H$ NMR spectra of [(6-$Ph_2$TPA)Ni(3-Hfl)]$ClO_4$ (**3**, top), [(6-$Ph_2$TPA)Ni(*O*-bs)]$ClO_4$ (**10**, middle) and **10** upon treatment with one equiv. of 3-Hfl in $CD_3CN$ (bottom).

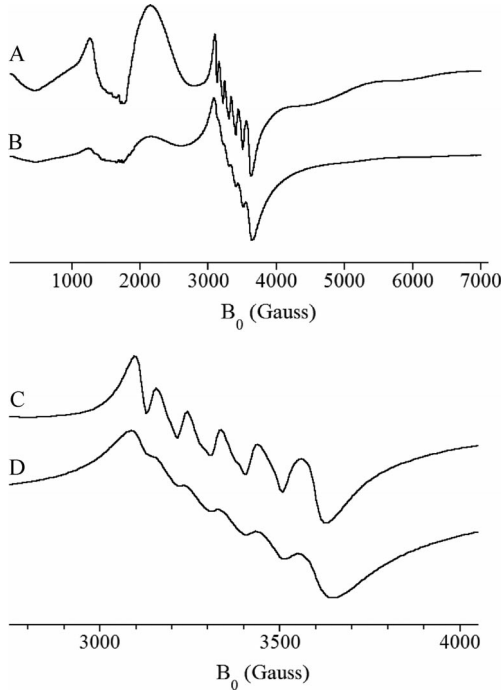


Figure 6. Top: X-band EPR spectra of **1** (A) and **8** (B). Conditions as noted in Exp. Sect. Bottom: expansion of the $g = 2$ region near 3500 G (C, D).

  

The $Co^{II}$ complexes **2** and **9** display EPR spectra (Figure 7) consistent with high-spin $Co^{II}$ in a site of moderate to low symmetry. The six-coordinate 3-hydroxyflavonolato-$Co^{II}$ complex **2** (Figure 7, top) gives the appearance of a simple rhombic spectrum, with $g^{eff}$ = [6.90, 2.08, 1.48] and poorly resolved $^{59}Co$ hyperfine coupling at low field [$A(^{59}Co)$ = 40 G]. Closer inspection of this spectrum shows weak features at $g^{eff}$ = 5.70 and 2.95 the intensity of which decays rapidly with temperature. Consistent with our prior observation of parallel mode responses in high-spin $Co^{II}$ systems,[19] this six-coordinate complex gives a relatively weak parallel mode signal, maximizing in intensity at high power and low temperature, at approximately 4.5% of the perpendicular mode signal. This value is slightly larger than observed for higher symmetry six-coordinate complexes, consistent with the heterogeneity of the first coordination sphere ($N_4O_2$ coordination) but clearly indicative of retention of the six-coordinate structure in solution.

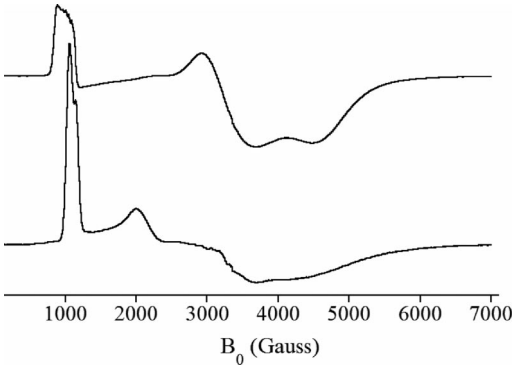


Figure 7. X-band EPR spectra of **2** (top) and **9** (bottom). Conditions as noted in the Exp. Sect.

The five-coordinate *O*-bs-$Co^{II}$ complex **9** gives a more complex low temperature EPR spectrum (Figure 7, bottom), with slightly less overall *g* anisotropy: the largest *g* value is 6.36 and the smallest is 1.53. However, this is clearly a less simple spectrum in appearance, with the largest *g* value split (6.36, with a shoulder at 5.95) and additional features at $g^{eff}$ = 3.36 and 2.03. Unlike the six-coordinate $Co^{II}$ flavonolato complex **2**, the appearance of the spectrum for the *O*-bs complex does not change significantly with increasing temperature. Attempts to simulate this signal as a simple effective $S' = {}^1/_2$ spin system gave only unsatisfactory results, failing to reproduce the features at $g^{eff}$ = 3.36 and 2.03 simultaneously. As noted above for the six-coordinate complex **2**, the five-coordinate *O*-bs complex **9** also gives a parallel mode response and this signal maximizes at 10.8% of the perpendicular mode signal, consistent with its formulation as a five-coordinate complex in solution.

The EPR spectrum of the enzyme/substrate (ES) complex for the $Co^{II}$-containing quercetinase from *Streptomyces sp. FLA* contains features at $g \approx 6$, 3.8 and 2.3.[5a] Exposure of a solution of the ES adduct to oxygen results in loss of this signal and the appearance of new features that may be for a product-bound species. Overall, the features exhibited by both species suggest that throughout the catalytic cycle of the enzyme, a tetrahedral or trigonal bipyramidal $Co^{II}$ center is maintained. In terms of the synthetic complexes **2** and **9**, the overall coordination number at the $Co^{II}$ center decreases from six to five on going from the flavonolato complex to the *O*-bs product.

The EPR spectrum of the *O*-bs-$Cu^{II}$ complex **11** is best described by a rhombic ***g*** tensor (***g*** = [2.01, 2.09, 2.25]) with resolved $^{63,65}Cu$ hyperfine coupling at all three *g* values (Figure 8). A nearly axial $^{63,65}Cu$ hyperfine tensor is indicated, ***A*** = [–180, –200, 360] MHz and the magnitude of the Cu hyperfine, in combination with a rhombic *g* tensor, obscures nearly all evidence of coordinated $^{14}N$. Their inclusion in the simulation (gray line in Figure 8) only serves to broaden the $^{63,65}Cu$ features, without offering any additional information. Consequently, we could not address the relative couplings to the axial and equatorial nitrogen donors. Interestingly, in solution at room temperature, some of the *g* anisotropy is preserved and a simple isotropic pattern was not observed, regardless of concentration or spectrometer conditions. All attempts to simulate this signal with the average *A* and *g* values obtained from the frozen solution spectroscopic simulation failed to reproduce the room temperature spectrum.

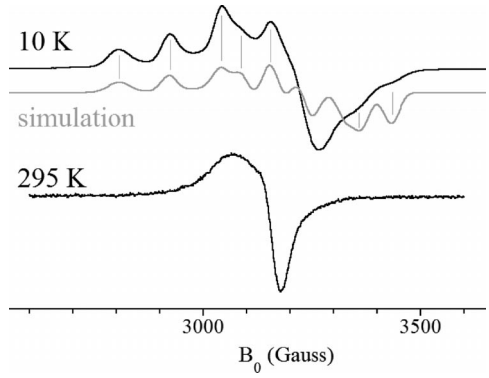


Figure 8. X-band EPR spectra of **11** in frozen (top) and fluid (bottom) solution. Conditions: temperature as noted; 2 G field modulation; microwave power: 0.2 mW (10 K) or 2 mW (295 K); all other conditions as noted in Exp. Sect. The gray line is a simulation of the low temperature spectrum using the following parameters: ***g*** = [2.01, 2.09, 2.25]; ***A***($^{63,65}Cu$) = [–180, –200, 360] MHz; 4 MHz *p*-p line width.

EPR studies of the $Cu^{II}$-containing quercetinase from *Aspergillus japonicus* revealed an ES complex with $g_{\|}$ = 2.366 and $A_{\|} \approx 110$ G.[20] These values place the copper center in a region of a Peisach-Blumberg plot between those typically occupied by type 1 and type 2 Cu sites.[21] After exposure of the solution of the ES complex to oxygen, a new EPR spectrum was obtained with *A* and *g* values suggestive of a copper(II) center having a distorted trigonal bipyramidal geometry. This species is proposed to be a product-bound complex, as the spectrum of the resting state enzyme can be regenerated after extensive washing of the enzyme with buffer. Differences in the EPR features of the $Cu^{II}$ flavonolato complex **4**[6] vs. those of the *O*-bs complex **11** provide evidence for structural perturbations at the $Cu^{II}$ center. The geometry of **4** is distorted square pyrami-

  

dal ($\tau$ = 0.11)[16] with the flavonolato ligand coordinated in the equatorial plane and a phenyl-appended pyridyl appendage of the 6-$Ph_2$TPA ligand that is not coordinated to the metal center. As X-ray quality crystals have not yet been obtained for **11**, the coordination motifs of the *O*-bs carboxylate moiety and the supporting chelate ligand in this complex are currently unknown.

### Evaluation of Photoinduced Catalytic Activity

Speier, et al. have previously reported that $Cu^{II}$ complexes of 3-Hfl can serve as catalysts for the oxidative degradation of the flavonol under thermal conditions.[2a] These reactions were typically performed in DMF solutions at 100 °C using a ratio of 1:5 to 1:20 (complex:flavonol). The percent conversion to *O*-bs and CO was determined for several complexes and ranged from 17–91%. The reaction catalyzed by [$Cu^{II}$(fla)(idpa)]$ClO_4$ {fla = flavonolate; idpa = 3,3′-iminobis(dimethylpropylamine)} was evaluated by means of kinetic studies as a function of complex and flavonol concentration and at different oxygen pressures.[22] These studies revealed that the rate-determining step is second-order overall, $-d[flaH]/dt = k$ [{$Cu^{II}$(fla)(idpa)}-$ClO_4$][$O_2$].

Biomimetic light-driven catalytic reactions are an area of significant current interest.[23] In this regard, we have evaluated the products generated upon irradiation ($\lambda_{irr}$ = 300 nm; 18 h) of oxygen-purged acetonitrile solutions of **1**–**4** containing 20 equiv. of 3-HflH. In each case, the flavonol is completely consumed and two organic products are generated, *O*-benzoylsalicylic acid (*O*-bsH, major) and a phthalide (minor) (Scheme 1; Table 2). The production of *O*-bsH as the major product indicates that the metal complex catalyzes photoinduced dioxygenase-type chemistry akin to the single turnover reactions described herein. Previous studies of the photochemistry of 3-HflH have shown that it instead undergoes a photoinduced isomerization reaction to give 3-hydroxy-3-phenyl-1,2-indandione,[11,24] followed by conversion to a 3-arylphthalide (Scheme 1).[25,26] While the full role of the metal center in enabling photoinduced single-turnover and catalytic dioxgenase-type reactivity for 3-HflH remains to be elucidated, with regard to catalysis, the metal center must facilitate protonation of the metal-bound *O*-bs ($pK_a \approx 3$) by 3-hydroxyflavonol ($pK_a \approx 7.8$; Scheme 1) through stabilization of the chelate anion of the latter. Independent experiments demonstrate that treatment of the *O*-bs complex [(6-$Ph_2$TPA)Ni(*O*-bs)]$ClO_4$ (**10**) with one equiv. of 3-hydroxyflavonol results in the rapid regeneration of a significant amount of the 3-Hfl complex **3** [Figure 2 ($^1$H NMR); Supporting Information, Figure S6 (UV/Vis)]. Similar regeneration of the 3-Hfl complexes is found for the other metal ions [$Co^{II}$: Figure 3 ($^1$H NMR); Figure S7 (UV/Vis); $Mn^{II}$ and $Cu^{II}$: Figures S8 and S9]. Overall, we propose a reaction pathway for photoinduced catalytic dioxygenase-type reactivity as shown in Scheme 1 (bottom).

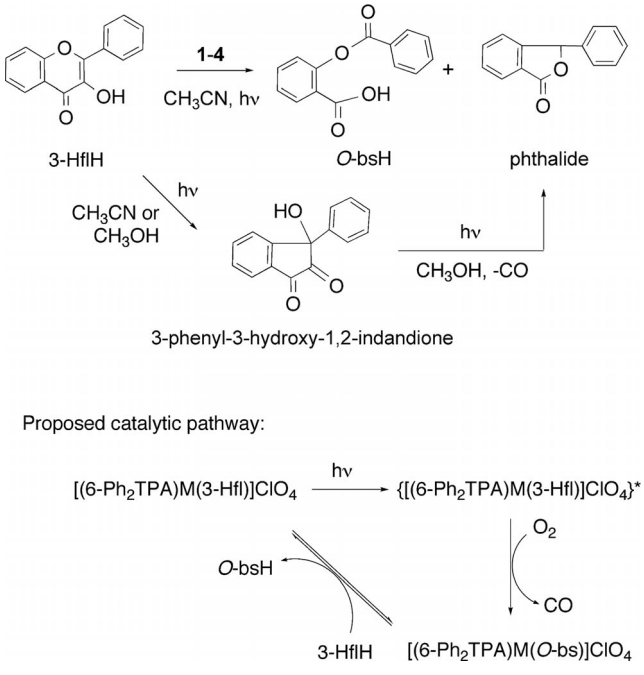


Scheme 1. (top) Reaction products generated in photoinduced reactions catalyzed by **1**–**4** and in the reaction of 3-HflH. (bottom) Proposed reaction pathway for metal-catalyzed oxidative ring-opening of 3-HflH.

Table 2. Percent yields of products generated in photoinitiated reactions catalyzed by **1**–**4**.

| | **1** | **2** | **3** | **4** |
|---|---|---|---|---|
| *O*-bsH | 62 | 52 | 63 | 60 |
| Phthalide | 10 | 17 | 7 | 13 |

## Discussion

The photochemistry of 3-HflH has previously been evaluated under a variety of conditions, most notably as a function of solvent. Matsuura, et al. performed studies in mixed 2-propanol/benzene solution using a high pressure Hg lamp. These reactions resulted in the formation of 3-hydroxy-3-phenyl-1,2-indandione in high yield.[24] Yokeo and coworkers subsequently showed that use of methanol as a solvent under similar conditions results in the formation of a mixture of the indandione and a phthalide (Scheme 1), the latter of which is the result of a photoinduced loss of carbon monoxide.[25] Performing the photoirradiation of 3-HflH in $CH_3CN$, Ficarra and coworkers found that only the indandione was obtained.[26] In our laboratory, we found that irradiation of a $CH_3CN$ solution of 3-HflH at 300 nm for 18 h produces the phthalide as the major product, even in the presence of oxygen. Photooxygenation of 3-HflH to produce *O*-bsH has been previously shown to occur in pyridine in the presence of the photosensitizer rose bengal.[27] The results presented herein show that the presence of a metal ion, whether under stoichiometric or catalytic conditions, promotes the photoinduced oxidative degradation of 3-HflH to produce *O*-bsH and CO as products.

To date, very few investigations of the photoinduced reactivity of metal-coordinated flavonolates have been re-

  

ported.[7,8] In the present study, we found that irradiation of 3-hydroxyflavonolato complexes of $Mn^{II}$, $Co^{II}$, $Ni^{II}$ and $Cu^{II}$ supported by the 6-$Ph_2$TPA ligands **1**–**4** at 300 nm results in CO release and the formation of the corresponding *O*-benzoylsalicylato complexes **8**–**11** which were isolated and comprehensively characterized. The identification of clean photoinduced dioxygenase-type chemistry for these complexes is akin to the chemistry we have identified for structurally similar complexes of the Group 12 metal ions **5**–**7**.[7] This reactivity differs from that reported for simple $Zn^{II}$, $Al^{III}$ and $Pb^{II}$ complexes of 3-Hfl generated in situ in methanol wherein, similar to the chemistry of the free flavonol, photoisomerization to give 3-hydroxy-3-phenyl-1,2-indandione was identified.[11a] The origin of these differences in reactivity has not yet been identified and studies directed at examining how factors such as the solvent (acetonitrile vs. methanol) influence the photoinduced reactivity of metal-coordinated flavonols are underway in our laboratory.

Complexes **1**–**4** can serve as catalysts for the photoinduced oxidative ring opening of 3-hydroxyflavonol. Speier et al. have previously shown that $Cu^{II}$ flavonolato complexes could also act as catalysts for the same reaction under thermal conditions (> 80 °C for at least 8 h for 20 turnovers).[2] As the photochemical processes occur under relatively mild conditions, our results suggest that the presence of metal ions in natural environments (e.g. plants) may enhance light-induced flavonol degradation and CO-release reactivity. It is worth noting that the supporting chelate ligand present in **1**–**4** may actually inhibit reactivity resulting from UV irradiation due to absorption of light in the same region.[28] With regard to metal/flavonol photochemistry, we note that Yokeo and coworkers have previously reported that the presence of metal ions such as $Co^{II}$, $Ni^{II}$ and $Cu^{II}$ prevents the photochemical rearrangement of flavonols.[25] Our results demonstrate that such metal centers promote oxidative cleavage reactivity, thereby limiting the amount of photoisomerization products generated.

In terms of CO-releasing compounds, our results indicate that metal flavonolato complexes are a new group of $O_2$-dependent, photoinduceable CO-releasing systems. The difference in photoinduced reactivity of closed shell (e.g. $Zn^{II}$)[7] complexes relative to that exhibited by the open-shell systems described herein indicates a level of tunability for the CO-release reaction.

## Experimental Section

**General Comments:** All reagents and solvents were obtained from commercial sources and were used as received unless otherwise noted. Dry solvents for glovebox use were prepared according to published procedures[29] and were distilled under $N_2$ prior to use. Air-sensitive reactions were performed in a MBraun Unilab or Vacuum Atmospheres glovebox under an $N_2$ atmosphere. The flavonolato complexes **1**–**4** were prepared as described previously.[6]

**Physical Methods:** UV/Vis spectra were recorded on a Hewlett–Packard 8453 diode array spectrophotometer. Fluorescence emission spectra were obtained using a Shimadzu RF-530XPC spectrometer in the range of 250–900 nm with the excitation wavelength corresponding to the absorption maximum of the complex above 400 nm. The excitation and emission slit widths were set at 5 nm for all experiments. Reaction quantum yield measurements were determined using actinometry with ferrioxalate as a standard to measure photon flux.[13] IR spectra were recorded on a Shimadzu FTIR-8400 spectrometer as KBr pellets. $^1$H NMR spectra of diamagnetic compounds were obtained on a Bruker ARX-400 or JEOL ECX-300 spectrometer and were referenced to the residual proton signal of the deuterated solvent. $^1$H NMR spectra of paramagnetic species were recorded on a Bruker ARX-400 spectrometer as described previously and the chemical shifts (in ppm) are reported relative to the residual solvent peak(s) in $CHD_2CN$ [$^1$H, 1.94 (quintet) ppm].[17] Elemental analyses were performed by Atlantic Microlabs Inc., Norcross, GA.

**EPR Spectroscopy:** Frozen solution X-band EPR spectra were recorded on a Bruker EMX EPR spectrometer equipped with either an ER-4102HS (perpendicular mode only) or an ER-4116DM dual mode resonator, with the temperature maintained by an Oxford ESR-900 liquid He cryostat. All samples were approximately 1 mM in 50:50 (v/v) toluene/dichloromethane and were thoroughly degassed by multiple freeze-pump-thaw cycles prior to data collection. Unless otherwise noted, the spectra presented herein were recorded using the following conditions: $T$ = 4.5 K; $\nu_{MW}$ = 9.38 GHz (0.2 mW); 5 G field modulation (100 kHz); receiver gain: $10^4$; time constant: 82 ms. $Cu^{II}$ spectra were simulated using the program EasySpin (available free of charge at www.easyspin.org).[30]

***Caution!*** Perchlorate salts of metal complexes with organic ligands are potentially explosive. Only small amounts of material should be prepared and these should be handled with great care.[31]

**Irradiation of 1–4 with UV Light. Isolation and Characterization of 8–11:** A solution of each complex (**1**–**4**, ca. $5 \times 10^{-3}$ M) was dissolved in acetonitrile (10 mL) and transferred to a round-bottomed flask. The flask was sealed with a septum and parafilm, purged with $O_2$ for 40 s and then inserted into a Rayonet photochemical reactor equipped with 300 nm lamps. The reaction progress was periodically evaluated using UV/Vis spectroscopy by measuring the intensity of the absorption of the metal-bound flavonolate at approximately 420–440 nm. After each reaction reached completion, the solvent was evaporated under reduced pressure. The remaining residue was then dissolved in a minimal amount of acetonitrile. Addition of excess diethyl ether resulted in the deposition of powders of **8**–**11**. Each powdered sample was subsequently dried under vacuum. Crystals of **9** suitable for a single-crystal X-ray diffraction study were obtained by diffusion at room temperature of diethyl ether into a dilute acetonitrile solution of the complex.

**[(6-$Ph_2$TPA)Mn(*O*-bs)]OTf·0.25$CH_2Cl_2$ (8):** Green/beige powder; yield 74%. $C_{45}H_{35}F_3MnN_4O_7S·0.25CH_2Cl_2$ (909.0): calcd. C 55.36, H 3.78, N 5.57; found C 55.48, H 4.00, N 5.76. FTIR (KBr): $\tilde{\nu}$ = 1736 ($\nu_{C=O}$) cm$^{-1}$. ESI/APCI-MS, *m*/*z* (%) 738.2049 ([M – OTf]$^+$, 1.8%).

**[(6-$Ph_2$TPA)Co(*O*-bs)]$ClO_4$·0.2$H_2O$ (9):** Green crystals; yield 88%. $C_{44}H_{35}ClCoN_4O_8·0.2H_2O$ (845.8): calcd. C 60.18, H 4.48, N 6.38; found C 60.45, H 4.22, N 6.26. FTIR (KBr): $\tilde{\nu}$ = 1736 ($\nu_{C=O}$) cm$^{-1}$. ESI/APCI-MS, *m*/*z* (%) 742.1982 ([M – $ClO_4$]$^+$, 100%).

**[(6-$Ph_2$TPA)Ni(*O*-bs)]$ClO_4$·2$H_2O$·0.6$CH_3CN$ (10):** Beige/pink powder; yield 78%. $C_{44}H_{35}ClN_4NiO_8·2H_2O·0.6CH_3CN$ (841.9+36.0+24.6): calcd. C 60.15, H 4.56, N 7.14; found C 60.57, H 4.34, N 7.46. FTIR (KBr): $\tilde{\nu}$ = 1736 ($\nu_{C=O}$) cm$^{-1}$. ESI/APCI-MS, *m*/*z* (%) 741.1995 ([M – $ClO_4$]$^+$, 100%).

**[(6-$Ph_2$TPA)Cu(*O*-bs)]$ClO_4$·3$H_2O$·0.9$CH_3CN$ (11):** Blue crystals; yield 85%. $C_{44}H_{35}ClCuN_4O_8·3H_2O·0.9CH_3CN$ (846.8+54.0+36.9):

  

calcd. C 58.66, H 4.70, N 7.32; found C 58.71, H 4.07, N 7.32. FTIR (KBr): $\tilde{\nu}$ = 1736 ($\nu_{C=O}$) $cm^{-1}$. ESI/APCI-MS, *m*/*z* (%) 746.1952 ($[M - ClO_4]^+$, 48%).

**Dark Control Reactions:** Foil covered, oxygen-purged $CH_3CN$ solutions of **1**–**4** were placed in the photoreactor for 18 h with 300 nm irradiation. Evaluation by $^1H$ NMR [$Co^{II}$ (**2**) and $Ni^{II}$ (**3**)] or UV/Vis spectroscopy [$Mn^{II}$ (**1**), $Co^{II}$ (**2**), and $Cu^{II}$ (**4**)] showed no reaction. These results provide evidence that the observed reactivity is photoinduced and not a thermal reaction.

**Anaerobic Control Reactions:** Nitrogen-purged $CH_3CN$ solutions of **1**–**4** were placed in the photoreactor for 18 h with 300 nm irradiation. Evaluation by $^1H$ NMR spectroscopy [$Co^{II}$ (**2**) and $Ni^{II}$ (**3**)] showed no reaction. Evaluation of the reactions involving the $Mn^{II}$ (**1**) and $Cu^{II}$ (**4**) complexes at low concentration (ca. $10^{-5}$) by UV/Vis showed an approximately 50% decrease in the 420–430 nm absorption band which may indicate $O_2$ leakage into the reaction or a slow background reaction.

**CO Quantification:** Gas chromatography (Agilent 3000A Micro GC with TCD detector) was used to quantify CO release from **3**. A calibration curve was developed using sodium formate/sulfuric acid. A glass vial containing a $CH_3CN$ solution of **3** (1.0 mL at 5.78 mM) was sealed with a septum and purged with $O_2$. After irradiation at 300 nm for 18 h the head space gas was examined by GC. Over a series of reactions, a maximum yield of approximately 50% was obtained for the production of one equiv. of CO. We attribute this less than quantitative yield of CO to partitioning between the solvent and headspace of the reaction vessel and to possible loss of CO through the septum during the 18 h of irradiation required for the reaction to reach completion.

**Catalytic Reactions. Spectroscopic Studies and Product Isolation:** 3-Hfl (20 mg; $8.4 \times 10^{-5}$ mol) was dissolved in acetonitrile (15 mL) and added to [$(Ph_2TPA)$M(3-Hfl)]$ClO_4$ (3.5 mg; where M = $Mn^{II}$, $Co^{II}$, $Ni^{II}$, $Cu^{II}$) solid. To this solution further acetonitrile (5 mL) was added to give a concentration of approximately $2.1 \times 10^{-5}$ M for the complex and $4.2 \times 10^{-4}$ M for [3-Hfl]. This mixture was then transferred to a 50 mL round-bottomed flask and capped with a septum. After purging the reaction mixture with $O_2$ for 40 s, the flask was placed in a UV reactor ($\lambda_{irr}$ = 300 nm) for 18 h. After this time, the solvent was removed under reduced pressure and the remaining solid was extracted with Hex/EA (2:1; 3 × 2 mL). The organic extracts were filtered through a Celite/glass wool plug and the filtrate was dried. The percentage of *O*-benzoylsalicylic acid and 3-phenylphthalide in the solid sample obtained (ca. 14 mg) were determined by $^1H$ NMR relative peak integration.

### X-ray Crystallography

A single crystal of **9**·0.25$CH_3CN$ was mounted on a glass fiber using a viscous oil and was then transferred to a Nonius Kappa CCD diffractometer for data collection at 150(1) K (Table 3). Methods for determination of cell constants and unit cell refinement have been previously reported.[32] The structure was solved using a combination of direct methods and heavy atoms using SIR 97. All non-hydrogen atoms were refined with anisotropic displacement coefficients. Complex **9**·0.25$CH_3CN$ crystallizes in the space group *C*2/*c* with three oxygen atoms of the perchlorate anion exhibiting disorder.

CCDC-866629 contains the supplementary crystallographic data for this paper (excluding structure factors). These data can be obtained free of charge from The Cambridge Crystallographic Data Centre via www.ccdc.cam.ac.uk/data_request/cif.

Table 3. Summary of X-ray data collection and parameters for 9·0.25$CH_3CN$.[a]

| | **9**·0.25$CH_3CN$ |
|---|---|
| Empirical formula | $C_{45}H_{36.50}ClCoN_{4.50}O_8$ |
| $M_r$ | 862.67 |
| Crystal system | monoclinic |
| Space group | *C*2/*c* |
| *a* [Å] | 31.0219(6) |
| *b* [Å] | 11.0735(2) |
| *c* [Å] | 23.9944(5) |
| *α* [°] | 90 |
| *β* [°] | 106.9654(10) |
| *γ* [°] | 90 |
| *V* [Å$^3$] | 7883.9(3) |
| *Z* | 8 |
| $D_c$ [Mg m$^{-3}$] | 1.454 |
| *T* [K] | 150(1) |
| Color | green |
| Crystal habit | prism |
| Crystal size [mm] | 0.30 × 0.28 × 0.15 |
| Diffractometer | Nonius KappaCCD |
| *μ* [mm$^{-1}$] | 0.566 |
| $2\theta_{max.}$ [°] | 55.00 |
| Completeness to *θ* [%] | 99.5 |
| Reflections collected | 16568 |
| Independent reflections | 9028 |
| $R_{int}$ | 0.0417 |
| Variable parameters | 544 |
| $R_1/wR_2$[b] | 0.0894/0.1330 |
| Goodness-of-fit [$F^2$] | 1.036 |
| $\rho_{max./min.}$ [e Å$^{-3}$] | 0.675/–0.624 |

[a] Radiation used: Mo-$K_\alpha$ ($\lambda$ = 0.71073 Å). [b] $R_1 = \Sigma \mid |F_o| - |F_c| \mid / \Sigma |F_o|$; $wR_2 = \{\Sigma[w(F_o^2 - F_c^2)^2]/[\Sigma(F_o^2)^2]\}^{1/2}$, where $w = 1/[\sigma^2(F_o^2) + (aP)^2 + bP]$.

**Supporting Information** (see footnote on the first page of this article): Absorption and emission spectra of **1**–**4**; absorption spectra of **8**–**11** upon treatment with one equivalent of 3-Hfl.

## Acknowledgments

The authors thank the National Science Foundation (NSF) for financial support (CHE-0848858 to L. M. B., CHE-0964806 to D. L. T., and CHE-0847132 to R. C. S.).

[1] a) S. C. Bischoff, *Curr. Opin. Clin. Nutr. Metab. Care* **2008**, *11*, 733–740; b) L. H. Cazarolli, L. Zanatta, E. H. Alberton, M. S. R. B. Figueiredo, P. Folador, R. G. Damazio, M. G. Pizzolatti, F. R. M. B. Silva, *Mini-Rev. Med. Chem.* **2008**, *8*, 1429–1440; c) A. W. Boots, G. R. M. M. Haenen, A. Bast, *Eur. J. Pharmacol.* **2008**, *585*, 325–337; d) M. Friedman, *Mol. Nutr. Food Res.* **2007**, *51*, 116–134; e) D. Amic, D. Davidovic-Amic, D. Beslo, V. Rastija, B. Lucic, N. Trinajstic, *Curr. Med. Chem.* **2007**, *14*, 827–845; f) T. P. T. Cushnie, A. J. Lamb, *Int. J. Antimicrob. Agents* **2005**, *26*, 343–356; g) T. P. Cushnie, A. J. Lamb, *Int. J. Antimicrob. Agents* **2011**, *38*, 99–107.

[2] a) J. S. Pap, J. Kaizer, G. Speier, *Coord. Chem. Rev.* **2010**, *254*, 781–793; b) J. Kaizer, E. Balogh-Hergovich, M. Czaun, T. Csay, G. Speier, *Coord. Chem. Rev.* **2006**, *250*, 2222–2233; c) A. Y. Malkhasian, M. E. Finch, B. Nikolovski, A. Menon, B. E. Kucera, F. A. Chavez, *Inorg. Chem.* **2007**, *46*, 2950–2952.

[3] G. Baráth, J. Kaizer, G. Speier, L. Párkányi, E. Kuzmann, A. Vértes, *Chem. Commun.* **2009**, 3630–3632; a) J. Kaizer, G. Baráth, J. Pap, G. Speier, M. Giorgi, M. Réglier, *Chem. Commun.* **2007**, 5235–5237.

  

[4] R. A. Steiner, K. H. Kalk, B. W. Dijkstra, *Proc. Natl. Acad. Sci. USA* **2002**, *99*, 16625–16630.

[5] a) H. Merkens, R. Kappl, R. P. Jakob, F. X. Schmid, S. Fetzner, *Biochemistry* **2008**, *47*, 12185–12196; b) M. R. Schaab, B. M. Barney, W. A. Francisco, *Biochemistry* **2006**, *45*, 1009–1016; c) B. Gopal, L. L. Madan, S. F. Betz, A. A. Kossiakoff, *Biochemistry* **2005**, *44*, 193–201.

[6] K. Grubel, K. Rudzka, A. M. Arif, K. Klotz, J. A. Halfen, L. M. Berreau, *Inorg. Chem.* **2010**, *49*, 82–96.

[7] K. Grubel, B. J. Laughlin, T. R. Maltais, R. C. Smith, A. M. Arif, L. M. Berreau, *Chem. Commun.* **2011**, *47*, 10431–10433.

[8] A flavonolato-$Cu^{I}$ complex has also been reported to undergo photoinduced decomposition in the presence of oxygen. However, the photoproducts were not identified. H. Kunkely, A. Vogler, *Chem. Phys. Lett.* **2001**, *338*, 29–32.

[9] B. E. Mann, *Top. Organomet. Chem.* **2010**, *32*, 247–285.

[10] R. Motterlini, L. E. Otterbein, *Nat. Rev. Drug Discovery* **2010**, *9*, 728–743.

[11] a) S. Protti, A. Mezzetti, C. Lapouge, J.-P. Cornard, *Photochem. Photobiol. Sci.* **2008**, *7*, 109–119; b) L. Jurd, T. A. Geissman, *J. Org. Chem.* **1956**, *21*, 1395–1401.

[12] J. R. Lakowicz. *Fluorescence Spectroscopy*, 3rd ed., Springer Science & Business Media, New York, NY, **2006**.

[13] a) C. G. Hatchard, C. A. Parker, *Proc. R. Soc. London Ser. A* **1956**, *23*, 518–536; b) H. J. Kuhn, S. E. Braslavsky, R. Schmidt, *Pure Appl. Chem.* **2004**, *76*, 2105–2146.

[14] T. H. Allen, W. S. Root, *J. Biol. Chem.* **1955**, *216*, 309–317.

[15] J. S. Pap, A. Matuz, G. Baráth, B. Kripli, M. Giorgi, G. Speier, J. Kaizer, *J. Inorg. Biochem.* **2012**, *108*, 15–21.

[16] A. W. Addison, T. N. Rao, J. Reedijk, J. van Rijn, G. C. Verschoor, *J. Chem. Soc., Dalton Trans.* **1984**, 1349–1356.

[17] E. Szajna, P. Dobrowolski, A. L. Fuller, A. M. Arif, L. M. Berreau, *Inorg. Chem.* **2004**, *43*, 3988–3997.

[18] a) E. Szajna-Fuller, K. Rudzka, A. M. Arif, L. M. Berreau, *Inorg. Chem.* **2007**, *46*, 5499–5507; b) E. Szajna-Fuller, B. M. Chambers, A. M. Arif, L. M. Berreau, *Inorg. Chem.* **2007**, *46*, 5486–5498.

[19] A. R. Marts, S. M. Greer, D. R. Whitehead, T. M. Woodruff, R. M. Breece, S. W. Shim, S. N. Oseback, E. T. Papish, F. E. Jacobsen, S. M. Cohen, D. L. Tierney, *Appl. Magn. Reson.* **2011**, *40*, 501–511.

[20] I. M. Kooter, R. A. Steiner, B. W. Dijkstra, P. I. van Noort, M. R. Egmond, M. Huber, *Eur. J. Biochem.* **2002**, *269*, 2971–2979.

[21] J. Peisach, W. E. Blumberg, *Arch. Biochem. Biophys.* **1974**, *165*, 691–708.

[22] L. Barhács, J. Kaizer, J. Pap, G. Speier, *Inorg. Chim. Acta* **2001**, *320*, 83–91.

[23] G. Knör, *Chem. Eur. J.* **2009**, *15*, 568–578.

[24] a) T. Matsuura, T. Takemoto, R. Nakashima, *Tetrahedron Lett.* **1971**, *12*, 1539–1540; b) T. Matsuura, T. Takemoto, R. Nakashima, *Tetrahedron* **1973**, *29*, 3337–3340.

[25] I. Yokeo, K. Higuchi, Y. Shirataki, M. Komatsu, *Chem. Pharm. Bull.* **1981**, *29*, 894–898.

[26] R. Ficarra, P. Ficarra, S. Tommasini, S. Campagna, G. Guglielmo, *Boll. Chim. Farm.* **1994**, *133*, 665–669.

[27] T. Matsuura, H. Matsushima, H. Sakamoto, *J. Am. Chem. Soc.* **1967**, *89*, 6370–6371.

[28] The photoisomerization of 3-HflH in acetonitrile is slower in the presence of 6-$Ph_2$TPA.

[29] W. L. F. Armarego, D. D. Perrin, *Purification of Laboratory Chemicals*, 4th ed., Butterworth-Heinemann, Boston, MA, **1996**.

[30] S. Stoll, A. Schweiger, *J. Magn. Reson.* **2006**, *178*, 42–55.

[31] W. C. Wolsey, *J. Chem. Educ.* **1973**, *50*, A335.

[32] E. Szajna, M. M. Makowska-Grzyksa, C. C. Wasden, A. M. Arif, L. M. Berreau, *Inorg. Chem.* **2005**, *44*, 7595–7605.

Received: March 1, 2012
Published Online: ■

  

EurJIC European Journal of Inorganic Chemistry

Enzyme Models

UV irradiation of 3-hydroxyflavonolato complexes of d*n* metal ions under aerobic conditions results in oxidative carbon–carbon bond cleavage and the formation of *O*-benzoylsalicylato complexes and CO under stoichiometric or catalytic conditions. These results show that a variety of metal ions promote light-induced flavonol oxidation and CO release under mild conditions.

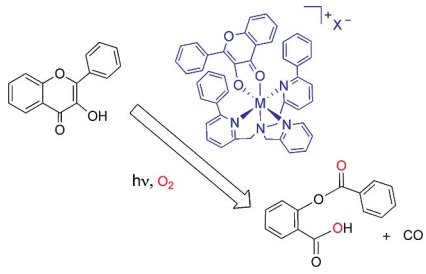




**Keywords:** Bioinorganic chemistry / Enzyme models / Homogeneous catalysis / Oxygen / Carbon monoxide

  